Hindawi
Shock and Vibration
Volume 2022, Article ID 6988292, 10 pages
https://doi.org/10.1155/2022/6988292

Research Article

Research on the Conversion Relationship between Dynamic Point Load Strength and Dynamic Compressive Strength Based on Energy System

Ming Zhou ,[1,2] Lan Qiao,[1] Qingwen Li ,[1] Shuang Yang,[1,2] and Zhenping Huang[1]

[1]*University of Science & Technology Beijing, Beijing, China*
[2]*Shunde Graduate School, University of Science and Technology Beijing, Foshan 528399, China*

Correspondence should be addressed to Qingwen Li; qingwenli@ustb.edu.cn

Received 13 December 2021; Revised 19 March 2022; Accepted 11 April 2022; Published 30 April 2022

Academic Editor: Xiaochen Wei

Point load test is a simple and fast method to obtain the compressive strength of rock. According to the maximum load at failure and the distance between two cone ends, the compressive strength of specimens can be calculated by the empirical formula. Because the test process does not need to process the sample into laboratory size type, so it is widely used. At the same time, with the rapid development of rock dynamics, the dynamic strength index of rock becomes more and more important under dynamic load. But dynamic point load is seldom mentioned by scholars. In order to explore the correlation between dynamic point load test and dynamic compressive strength, a large number of dynamic point load and uniaxial dynamic compressive strength tests were carried out using a split Hopkinson pressure bar for granite. Based on the energy theory, the crushing energy consumption during dynamic point load and uniaxial dynamic compressive strength tests were statistically analyzed, and the transformational relation between uniaxial dynamic compressive strength and crushing energy consumption during the dynamic point load test was determined. At the same time, the influence of the cone angle on crushing energy consumption during the dynamic point load test was investigated by changing the conical angle. The results show that with the increase in conical angle, the energy consumption of rock crushing decreases gradually during the dynamic point load test. And the decreasing trend tends to be gentle. The conclusion can provide a reference for obtaining the numerical value of the dynamic compressive strength of the rock in the future.

1. Introduction

Point load test is a simple method to test the compressive strength of rock, concrete, or other natural building materials under point load. Scholars at home and abroad have also made many research achievements on point load test. Koncagül and Santi [1] first proposed the idea of using irregular blocks to carry out point load test. Later, in 1972, the Committee of the International Society for Rock Mechanics recommended the use of the rock point load strength test method, and in 1985, it proposed a revised method to calculate the uniaxial compressive strength of rock, which has been widely recognized by most scholars [2]. Since then, in terms of point loads, a large number of scholars have studied it from different angles and different lithologies, including the relationship between point load strength and uniaxial compressive strength [3–9] and the determination of correction coefficient [10–14]. For example, D'Andrea et al. [15] were the first to indirectly estimate the uniaxial compressive strength of rock through a linear relationship, pointing out the linear correlation between point load strength index and uniaxial compressive strength. Franklin [2] found that the results of the unconfined uniaxial compressive strength test were closely related to the results of point load strength test, and the dispersion of the radial point load test was small. They described the development of a portable testing machine and suggested a conversion coefficient of 24. Bieniawski [16] evaluated the strength changes of three loading methods (axial test, radial test, and irregular test), found that the radial point load test was the most convenient to use, established the relationship between the three uniaxial compressive strength and point load index, and compiled a simple dimensional correlation diagram. All these proved the importance of point load-related research. The above studies were only for static point load test and static uniaxial compressive strength. However, with the rapid development of rock dynamics, dynamic load engineering problems such as deep mining, high slope blasting, and long tunnel (cave) excavation occurred, and dynamic compressive strength plays an important role in application [5, 17–20]. Therefore, it is of great significance to study whether the corresponding dynamic compressive strength can be determined through the dynamic point load test and how the transformation relationship between them. In terms of crack initiation and propagation, Haeri et al. [21] studied the fundamental failures occurring in a rock bridge. At the same time, the crack initiation, propagation, and rupture process of the CSCBD specimen under diameter compression were analyzed, tested, and simulated numerically. [22] Sarfarazi et al. [23] used the PFC2D method to study the influence of joint separation on the shear behavior of nonpersistent planar joints under high normal loads. And they compared stress-strain model prediction and test results for marble, sandstone, and dense Cambrian. The comparison showed that the model can accurately reproduce the mechanical behavior of rock. [24] In terms of impact research, Kumar [25] first applied the SHPB device to the test of rock dynamic strength in 1968. Bunshah [26] obtained the dynamic compression stress-strain curves of many metal materials in the range of strain rate $102\,s^{-1}$–$103\,s^{-1}$ through a large number of tests. Zhou et al. [27] found that the dynamic compressive strength increases first, then decreases slowly, and at last drops rapidly with the increase in prestress and found that for each water content, the dynamic tensile strength of sandstone is positively sensitive to loading rate by dynamic Brazilian disc experiments [28]. Janach [29] conducted impact tests on limestone and granite using the SHPB test facility, and the results also showed that the two kinds of rock dynamic strength are much higher than the static uniaxial compressive strength. These studies [30–36] promoted the focus of point load research from static mechanics to dynamic mechanics test and provided ideas for the transformation from static point load test to dynamic point load in this paper. In terms of the improvement of impact device, Chang [37] proposed the formula of penetration depth by using a simplified impact model, mechanics principle, and Bayesian statistical analysis of test data. Haldar and Hamieh [38] proposed an expression for the estimation of penetration depth based on data collation and analysis. The above research [39–42] provides thought support for the modification of the impact rod end of the SHPB impact device.

To sum up, there were only studies on static tests to calculate the compressive strength by using point load strength, and there were few studies on whether the dynamic compressive strength can be converted by point load test. In the Hopkinson impact experiment, there are few precedents of conical contact impact. This paper takes granite as the research object, carries out a dynamic impact compression test and dynamic point load test with a split Hopkinson pressure bar, and analyzes the crushing energy consumption in the two tests, respectively. Since the dynamic point load test cannot accurately calculate the strain rate, impact velocity is used as the medium. The relationship between impact velocity and crushing energy consumption in the impact compression test and that between impact velocity and dynamic point load test were fitted. Then, the proportion of crushing energy consumption in the dynamic point load test and dynamic compression test is determined. At the same time, the influence of different punch shapes on crushing energy consumption during the dynamic point load test was discussed by changing the cone angle of impact bar ends. Finally, the conversion relationship between the dynamic point load test crushing energy consumption and dynamic compression test crushing energy consumption under different conditions (different conical angles) was obtained by fitting.

2. Test Plan

2.1. Instrument and Method of Use. The dynamic uniaxial compression test adopts a split Hopkinson pressure bar (as shown in Figure 1). The diameter of the pressure bar is 50 mm, its elastic modulus E is 210 GPa, density is 7787 kg/m^3, wave velocity is 5667 m/s, the bullet is a spindle bullet of 0.26 m, and the length of the steel bar is 1.5 m. When testing, pay attention to the following experimental operation details: Both ends of the sample are fully coupled with grease to avoid mass reflection or consumption at the end due to insufficient transport medium. After the test began, the impact pressure was controlled to control the impact velocity, and the waveform of the incident, reflection, and transmission was collected by ultradynamic acquisition instrument.

The dynamic point load test is conducted by adding a self-designed point load impact rod head at one end of the incident bar (as shown in Figure 2). During the test, one end of the transmission bar was covered with a protective sleeve to prevent the impact rod head from continuing to damage the transmission bar after the sample was broken under the condition of a high strain rate. At the same time, the inside of the impact bar and the protection bar is coupled with the corresponding rod through grease. At the end of the test, the impact velocity was recorded, and the fragments and debris of the crushed sample were collected.

2.2. Preparation of Samples. The rock samples used in the test were all taken from the same large mine. In order to reduce the influence of nonuniformity on the test results, all samples in the test were cut from a complete granite block without obvious cracks. In the process of machining, the whole rock sample was cut into 32 standard patterns, which were divided into two groups for the dynamic point load test and impact compression test, respectively. Part of the sample is shown in Figure 3.

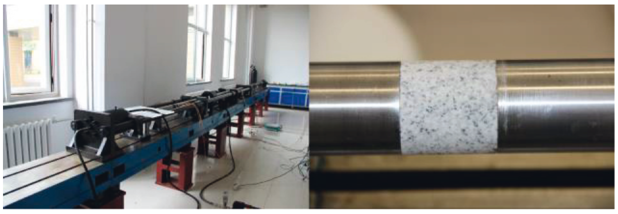

Figure 1: Split Hopkinson pressure bar test device.

Figure 2: Dynamic point load test bar and sample installation.

3. Test Results and Analysis

3.1. Data Processing

3.1.1. Acquisition of Crushing Energy Consumption for Dynamic Uniaxial Compressive Strength Test. Figure 4 shows the schematic diagram of the SHPB impact compression test. According to the above one-dimensional elastic wave hypothesis and stress-strain uniformity hypothesis, the stress $\sigma_s(t)$, strain rate $\dot{\varepsilon}_s(t)$, and strain $\varepsilon_s(t)$ of the sample are as follows:

$$\sigma_s(t) = \frac{EA_0}{2A_s}\left[\varepsilon_i(t) + \varepsilon_r(t) + \varepsilon_t(t)\right], \quad (1)$$

$$\varepsilon_s(t) = \frac{C_0}{l_s}\left[\varepsilon_i(t) - \varepsilon_r(t) - \varepsilon_t(t)\right], \quad (2)$$

$$\varepsilon_s(t) = \frac{C_0}{l_s}\int_0^t \left[\varepsilon_i(t) - \varepsilon_r(t) - \varepsilon_t(t)\right]\mathrm{d}t, \quad (3)$$

$$W_i = \frac{A_0 C_0}{E}\int \sigma_i^2 \mathrm{d}t = A_0 C_0 E \int_0^t \varepsilon_i^2 \mathrm{d}t, \quad (4)$$

$$W_r = \frac{A_0 C_0}{E}\int \sigma_r^2 \mathrm{d}t = A_0 C_0 E \int_0^t \varepsilon_r^2 \mathrm{d}t, \quad (5)$$

$$W_t = \frac{A_0 C_0}{E}\int \sigma_t^2 \mathrm{d}t = A_0 C_0 E \int_0^t \varepsilon_t^2 \mathrm{d}t, \quad (6)$$

$$W_a = W_i - W_r - W_t, \quad (7)$$

where A_s is the cross-sectional area of the test block; l_s is the initial length of the test block; A_0 is the cross-sectional area of the bar; C_0 is the propagation velocity of stress wave in the bar; E is the elastic modulus of the pressure bar; σ_i, ε_i is the stress and strain of the incident bar; σ_r, ε_r is the stress and strain of the reflecting bar; σ_t, ε_t is the stress and strain of the transmission bar; W_i is the incident energy; W_r is the reflection energy; W_t is the transmission energy; and W_a is the energy consumption of the broken.

Figure 5 shows the signal of the half-sine stress wave in a typical sample test. The three-wave method is used to verify the stress balance state during data processing. When the superposition curves of the incident and reflected waves and transmitted waves change from discoincidence to coincidence and then to discoincidence, it can be considered that the sample is in a state of stress balance in the process of dynamic loading.

The uniaxial impact compression experiment of typical granite was carried out by the SHPB system. The data are shown in Table 1. The crushing forms and stress-strain curves of granite under the SHPB experimental system are shown in Figures 6 and 7, respectively.

It can be seen from Figures 6 and 7 that the crushing scale and dynamic elastic modulus and peak stress of granite all show obvious strain rate effect. With the increase in strain rate, the crushing size decreases, and the dynamic elastic modulus and peak stress all show an increasing trend with the increase in strain rate. The rock has a strain rate effect, and the dynamic mechanical strength of intact granite samples is different under different strain rates. The dynamic compressive strength of rock increases with the increase in strain rate and impact velocity. For granite, when the stress reaches the yield stress, the stress-strain curve enters a significant plastic deformation stage with the increase in strain, and there is only a small plastic deformation stage before and after the peak stress. Microscopically, this phenomenon corresponds to a series of stages of the adiabatic shear process. The dynamic stress-strain relationship of rock with complex morphology is actually a comprehensive reflection of the strain hardening effect, strain rate strengthening effect, and thermal softening effect caused by adiabatic temperature rise.

In this paper, W_a is used to represent the crushing energy consumption in the impact compression test, $W_{a(60^\circ)}$ represents the crushing energy consumption in the point load test, where (60°) represents that the conical angle selected in the point load test is 60°. The following figure shows the energy time-history curves of several groups of typical impact compression tests, as shown in Figure 8. As can be seen from the figure, with the increase in impact velocity, the incident energy of granite increases, and so does the crushing energy consumption. A second-order fitting was carried out between the crushing energy consumption of the sample and the corresponding impact velocity, as shown in Figure 9. The fitting formula is as follows: $W_a = 5.08v^2 - 102.24v + 555.4$, and the determination coefficient R^2 is 0.98, indicating a good fitting degree. The crushing energy consumption of the impact compression test was fitted with the corresponding dynamic uniaxial compressive strength, as shown in Figure 10. The fitting formula is $W_a = 1.176\sigma - 113.694$, and the determination coefficient R^2 is 0.89.

3.1.2. Energy Consumption of Crushing for Dynamic Point Load Test. When the SHPB device is used for the test, the $\sigma - \varepsilon - \dot{\varepsilon}$ relationship of the sample needs to meet certain assumptions. For example, the whole system should be in a

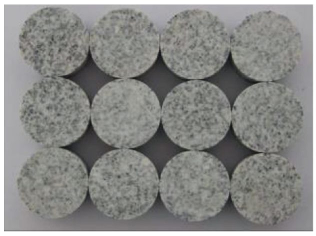

Figure 3: Test sample.

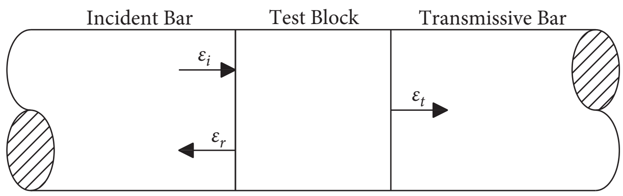

Figure 4: Schematic diagram of SHPB impact compression test loading.

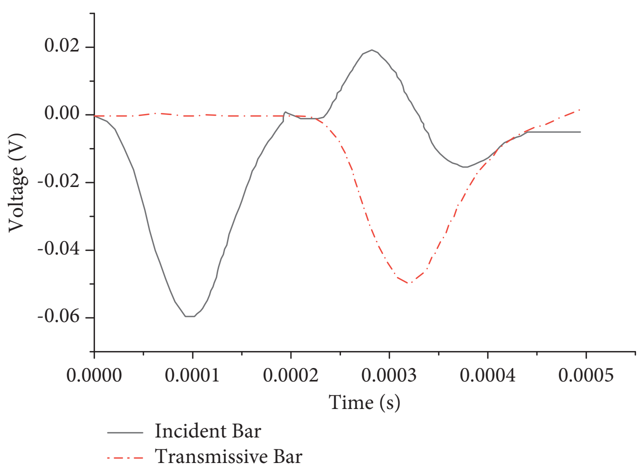

Figure 5: Electrical signal diagram of the typical sample during the experiment.

Table 1: Uniaxial impact compression test data.

Sample number	$V/m\cdot s^{-1}$	W_i/J	σ/MPa	W_a/J
1	9.78	94.82	129.33	41.65
2	10.32	95.01	132.03	41.7
3	10.79	95.27	137.43	41.95
4	11.4	119.87	140.32	49.23
5	12.07	142.29	146.60	64.31
6	12.60	157.33	158.57	71.93

one-dimensional stress state. After the stress wave is reflected several times in the specimen, the stress at the interface between the specimen and the elastic bar should be uniform. The friction effect at the junction between the specimen and the bar should be small enough to be ignored. However, for the dynamic point load test, the conical punch is installed at one end of the rod, so the stress uniformity cannot be achieved at the two interfaces between the specimen and the elastic rod, and the traditional calculation principle is not applicable. Therefore, the three-wave formula mentioned above cannot be used to calculate the stress, strain, and strain rate of specimens in the dynamic point load test. In the dynamic point load test, the bullet impacts the incident bar, the energy is transferred in the form of stress wave in the incident bar, and the energy is incident energy. Then, the stress wave is transmitted to the specimen, and the specimen is damaged. At this time, part of the stress wave is reflected as reflected wave, and the energy it has is called reflected energy. The other part of the stress wave is transmitted to the transmission rod through the specimen and becomes the transmitted wave. The energy it has is called the transmitted energy. When the energy absorbed by the specimen exceeds the energy required for the development of defects, new cracks will be generated in the specimen, and these cracks will gradually expand to all specimens. The original defects of the specimen and the new cracks will merge together, finally leading to the breakage of the specimen. In equations (4), (5), and (6), the parameters used in the energy calculation formula are incident strain ε_i, reflected strain ε_r, and transmitted strain ε_t, which are obtained from the data collected by strain gauge and do not involve the calculation principle of impact compression. Therefore, the above formula can be used to calculate the crushing energy consumption of samples in the dynamic point load test. Since the cone angle is 60 degrees in the standard static point load test, we also use a cone angle of 60 degrees in the dynamic point load to facilitate comparison with the test results of the static test. At the same time, the influence of different cone angles on crushing energy consumption in the test process will be further analyzed. The figure below shows the energy time-history curve of the dynamic point load test at different impact velocities when the cone angle of impact bar end is 60°.

Since the dynamic point load test does not meet the application conditions of the three-wave formula, the strain rate cannot be calculated, so the impact velocity is used as the measuring medium. As can be seen from Figure 11 and Table 2, with the increase in impact velocity, incident energy of the dynamic point load test increases, and so does crushing energy consumption. The crushing energy consumption of the sample was linearly fitted with the corresponding impact velocity, as shown in Figure 12. The fitting formula is as follows: $W_{a(60^{\circ})} = 14.25v - 66.37$, and the determination coefficient R^2 is 0.99, indicating a good fitting degree.

The relationship between the impact velocity and the energy consumption in the impact compression test (Figure 9) and the relationship between the impact velocity and the energy consumption in the dynamic load test (Figure 12) will be fitted again. Then, the relationship between energy consumption of impact compression test and dynamic load test is obtained, as shown in Figure 13, fitting formula is $W_a = 1.08W_{a(60^{*})} + 36.87$, and coefficient of determination R^2 is 0.9. Insert the fitting formula of W_a and dynamic compressive strength above into the formula to obtain $\sigma = 0.918W_{a(60^{*})} + 128.687$. In the formula, σ is the dynamic compressive strength, and $W_{a(60^{*})}$ is the crushing energy consumption in the dynamic point load test.

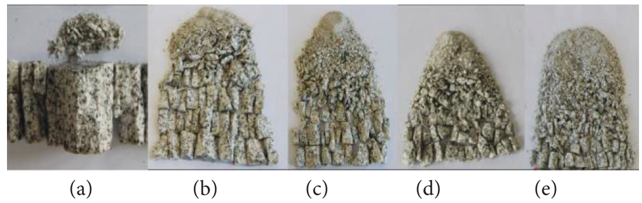

FIGURE 6: Degree and form of breakage of granite under different strain rates: (a) 68.3 s^{-1}, (b) 83.2 s^{-1}, (c) 124.9 s^{-1}, (d) 134.2 s^{-1}, and (e) 142.5 s^{-1}.

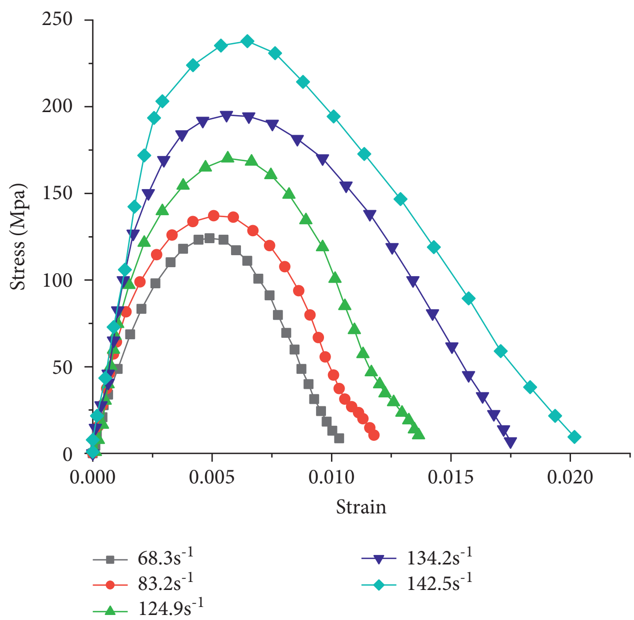

FIGURE 7: Dynamic compressive stress-strain curves of rock at different strain rates.

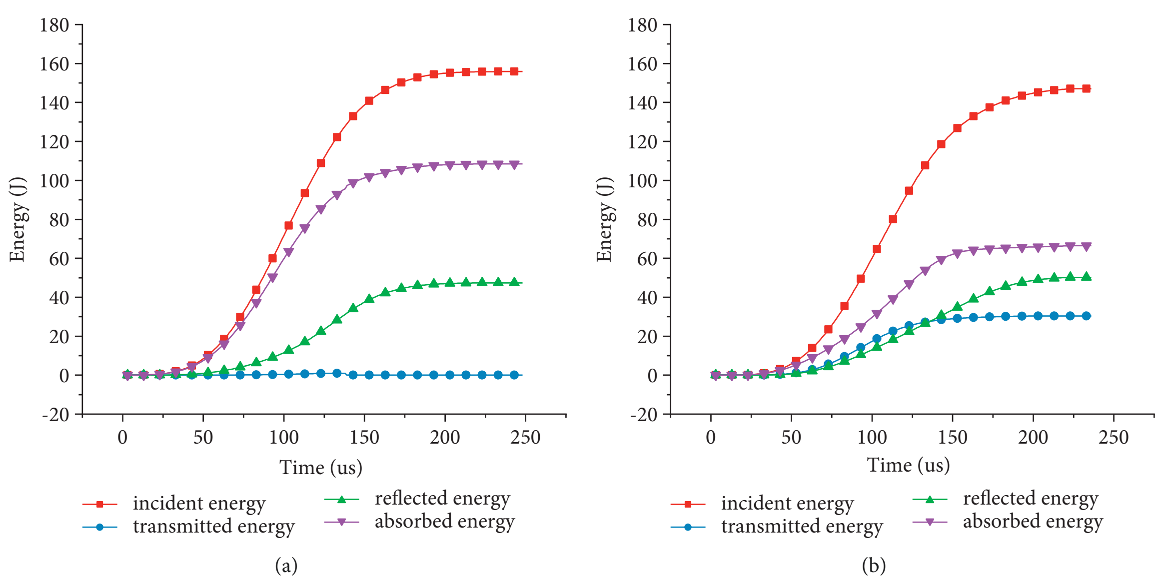

FIGURE 8: Continued.

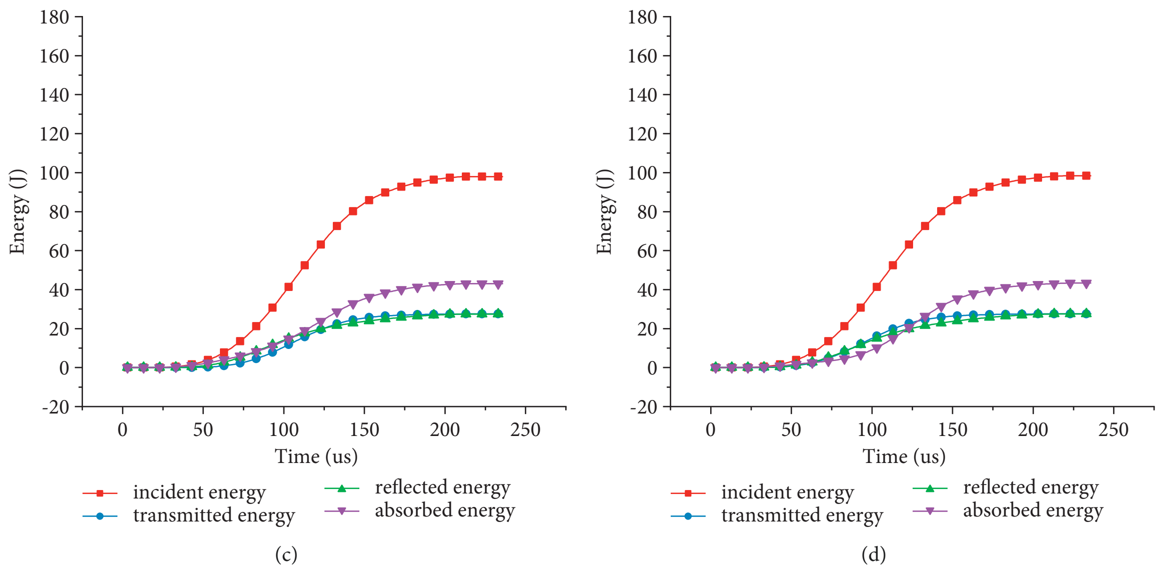

FIGURE 8: Energy time history curve of impact compression test. (a) Impact velocity 12.60 m/s. (b) Impact velocity 12.07 m/s. (c) Impact velocity 10.79 m/s. (d) Impact velocity 9.78 m/s.

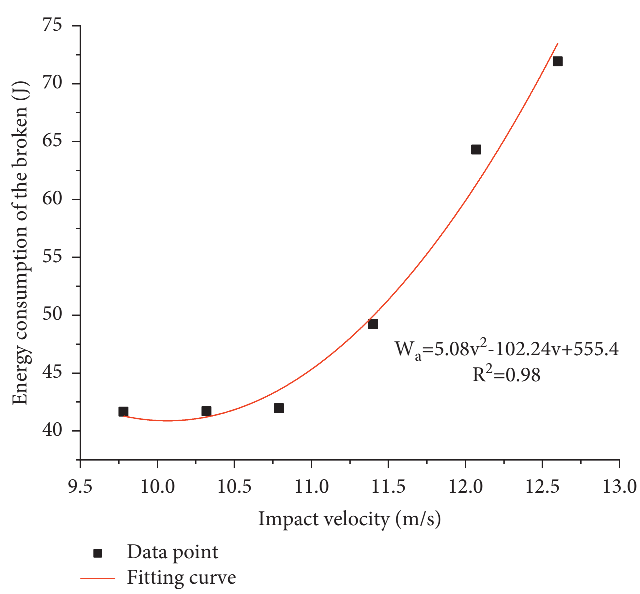

FIGURE 9: Fitting curve of crushing energy consumption-impact velocity in impact compression test.

3.1.3. Influence of Cone Angle on Crushing Energy Consumption during Dynamic Point Load Test. Two groups of dynamic point load impact tests were carried out by changing the cone angle to 90° and 120°. The relationship between impact velocity and crushing energy consumption in the experimental process was compared with that in the impact compression experiment. Figure 14 shows the fitting curves of dynamic point load crushing energy consumption and impact compression crushing energy consumption at three conical angles. As can be seen from the figure, when the cone angle is equal to 60° of the loading angle of the standard static point load test instrument, the crushing energy consumption of the dynamic point load test reaches maximum. With the

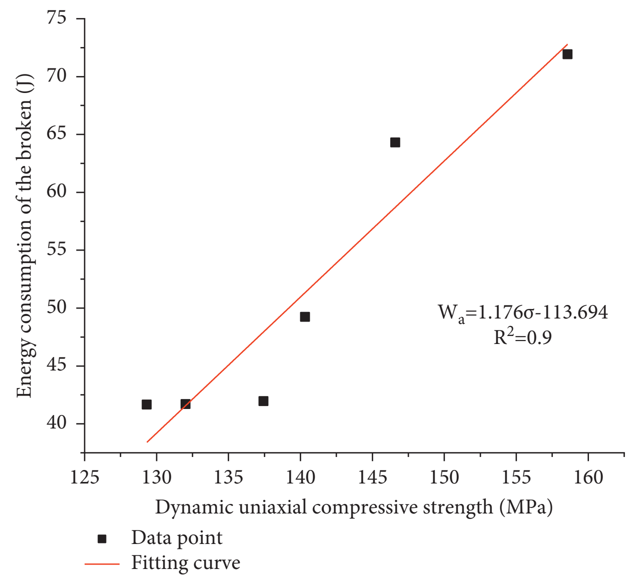

Figure 10: Fitting curve of crushing energy consumption-dynamic compressive strength.

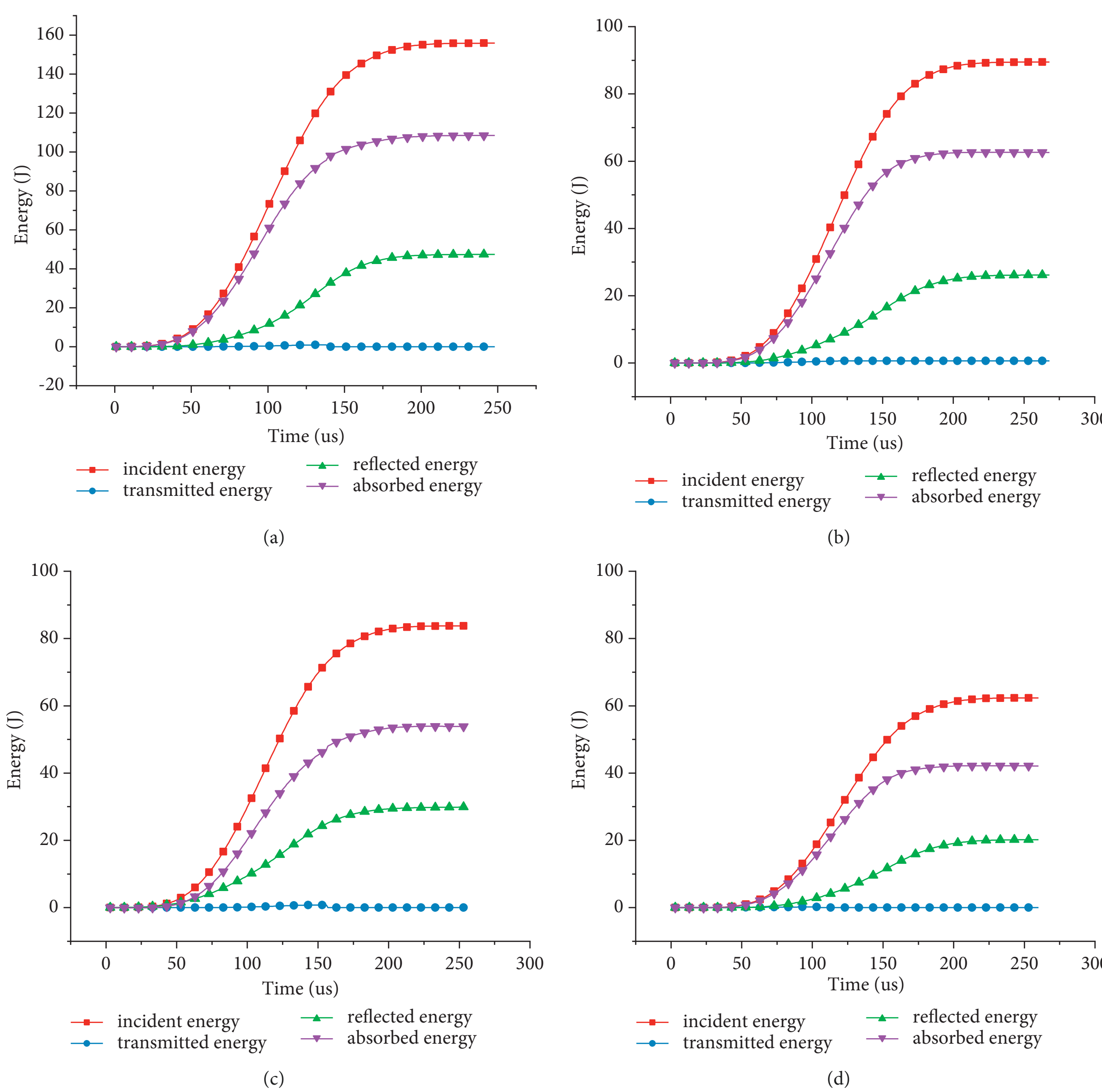

Figure 11: Energy time-history curve of the dynamic point load test at the conical angle of 60°. (a) Impact velocity 11.86 m/s. (b) Impact velocity 8.97 m/s. (c) Impact velocity 8.63 m/s. (d) Impact velocity 7.25 m/s.

Table 2: Test data of dynamic point load test at the conical angle of 60°.

Sample number	$V/m\cdot s^{-1}$	W_i/J	$W_{a(60°)}/J$
1	7.25	60.33	40.55
2	8.63	81.04	51.34
3	8.97	86.58	60.60
4	10.23	111.23	81.11
5	11.86	150.85	104.05
6	12.27	160.74	107.96

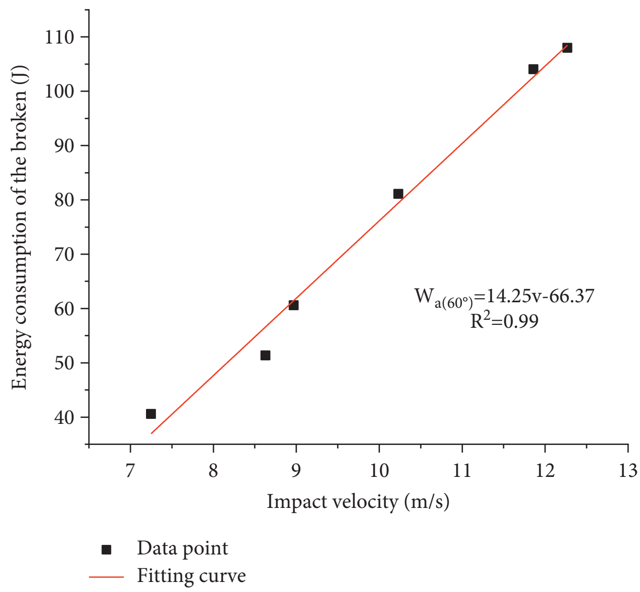

Figure 12: Fitting curve of crushing energy consumption-impact velocity of dynamic point load test at conical angle of 60°.

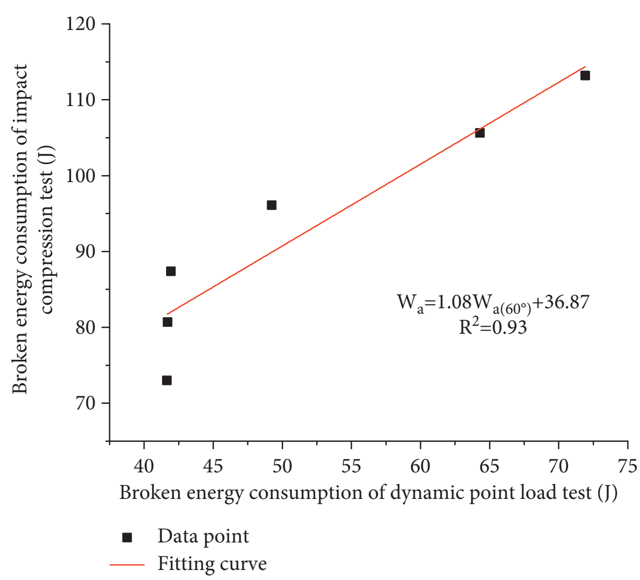

Figure 13: Fitting curve of crushing energy consumption of impact compression test-crushing energy consumption of dynamic point load test at conical angle of 60°.

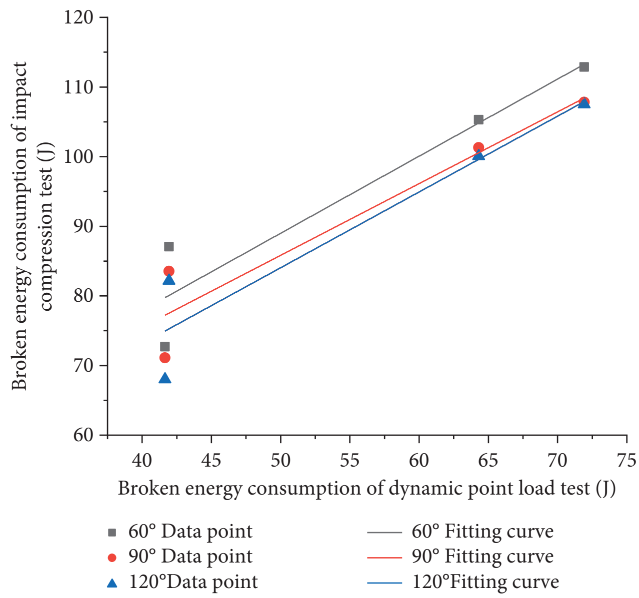

Figure 14: Comparison diagram of crushing energy consumption of load test at different conical angle points.

increase in cone angle, the crushing energy consumption of the dynamic point load test gradually decreases, and the decrease trend tends to be gentle.

4. Conclusions and Future Work

The research results are as follows:

(i) In the impact compression test, the crushing scale, dynamic elastic modulus, and peak stress of granite all show an obvious strain rate effect. With the increase in strain rate, the crushing size decreases, and the dynamic elastic modulus and peak stress all show an increasing trend with the increase of strain rate.

(ii) There is a certain proportion between the crushing energy consumed in the impact compression test and that consumed in the dynamic point load test: $W_a = 1.08W_{a(60^*)} + 36.87$. The relationship between uniaxial dynamic compressive strength and crushing energy consumption during the dynamic point load test is approximately as follows: $\sigma = 0.918W_{a(60^*)} + 128.687$. It can provide a reference for obtaining the value of dynamic compressive strength of rock on site in the future.

(iii) When the dynamic point load test is carried out, the cone angle has an effect on the crushing energy consumed during the test. When the cone angle is greater than 60° of the loading angle of the standard static point load test instrument, the larger the cone angle, the smaller the crushing energy consumption in the test, and the decrease trend tends to be gentle.

Data Availability

Some or all data, models, or code generated or used during the study are available from the corresponding author by request.

Conflicts of Interest

The authors declare that they have no conflicts of interest.

Acknowledgments

This work was supported by the National Natural Science Foundation of China and Shandong Province joint program (U1806209) and the Basic Scientific Research Operating Expenses of Central Universities (FRF-TP-19-021A3 and FRF-IDRY-19-002) and Scientific and Technological Innovation Foundation of Foshan (BK20BE008).

References

[1] E. C. Koncagül and P. M. Santi, "Predicting the unconfined compressive strength of the Breathitt shale using slake durability, shore hardness and rock structural properties," *International Journal of Rock Mechanics and Mining Sciences*, vol. 36, no. 2, pp. 139–153, 1999.

[2] J. A. Franklin, "Suggested method for determining point load strength," *International Journal of Rock Mechanics and Mining Sciences & Geomechanics Abstracts*, vol. 22, no. 2, pp. 51–60, 1985.

[3] H. Ozturk and M. Altinpinar, "The estimation of uniaxial compressive strength conversion factor of trona and interbeds from point load tests and numerical modeling," *Journal of African Earth Sciences*, vol. 131, pp. 71–79, 2017.

[4] T. N. Singh, A. Kainthola, and A. Venkatesh A, "Correlation between point load index and uniaxial compressive strength for different rock types," *Rock Mechanics and Rock Engineering*, vol. 45, no. 2, pp. 259–264, 2012.

[5] R. H. C. Wong, K. T. Chau, J.-H. Yin, D. T. W. Lai, and G.-S. Zhao, "Uniaxial compressive strength and point load index of volcanic irregular lumps," *International Journal of Rock Mechanics and Mining Sciences*, vol. 93, pp. 307–315, 2017.

[6] D. K. Ghosh and M. Srivastava, "Point-load strength: an index for classification of rock material," *Bulletin of the International Association of Engineering Geology*, vol. 44, no. 1, pp. 27–33, 1991.

[7] S. Kahraman, "Evaluation of simple methods for assessing the uniaxial compressive strength of rock," *International Journal of Rock Mechanics and Mining Sciences*, vol. 38, no. 7, pp. 981–994, 2001.

[8] D. Li and L. N. Y. Wong, "Point load test on meta-sedimentary rocks and correlation to UCS and BTS," *Rock Mechanics and Rock Engineering*, vol. 46, no. 4, pp. 889–896, 2013.

[9] J. Zhao and H. B. Li, "Experimental determination of dynamic tensile properties of a granite," *International Journal of Rock Mechanics and Mining Sciences*, vol. 37, no. 5, pp. 861–866, 2000.

[10] M. Koohmishi and M. Palassi, "Evaluation of the strength of railway ballast using point load test for various size fractions and particle shapes," *Rock Mechanics and Rock Engineering*, vol. 49, no. 7, pp. 2655–2664, 2016.

[11] L. A. Panek and T. A. Fannon, "Size and shape effects in point load tests of irregular rock fragments," *Rock Mechanics and Rock Engineering*, vol. 25, no. 2, pp. 109–140, 1992.

[12] J.-H. Yin, R. H. C. Wong, K. T. Chau, D. T. W. Lai, and G.-S. Zhao, "Point load strength index of granitic irregular lumps: size correction and correlation with uniaxial compressive strength," *Tunnelling and Underground Space Technology*, vol. 70, pp. 388–399, 2017.

[13] A. Mahmoodzadeh, M. Mohammadi, H. H. Ibrahim et al., "Artificial intelligence forecasting models of uniaxial compressive strength," *Transportation Geotechnics*, vol. 27, 2021.
[14] N. Turk and W. R. Dearman, "Improvements in the determination of point load strength," *Bulletin of the International Association of Engineering Geology*, vol. 31, no. 1, pp. 137–142, 1985.
[15] D. V. D'Andrea, R. L. Fischer, and D. E. Fogelson, "Prediction of compression strength from other rock properties," *Colorad Sch Min Q*, vol. 59, no. 4B, pp. 623–640, 1964.
[16] Z. T. Bieniawski, "The point-load test in geotechnical practice," *Engineering Geology*, vol. 9, no. 1, pp. 1–11, 1975.
[17] A. Basu and M. Kamran, "Point load test on schistose rocks and its applicability in predicting uniaxial compressive strength," *International Journal of Rock Mechanics and Mining Sciences*, vol. 47, no. 5, pp. 823–828, 2010.
[18] P. Asem and P. Gardoni, "A generalized Bayesian approach for prediction of strength and elastic properties of rock," *Engineering Geology*, vol. 289, Article ID 106187, 2021.
[19] P. Feng, F. Dai, Y. Liu, and X. Nuwen, "Effects of coupled static and dynamic strainratesonmechanical behaviors ofrock-like specimens containing pre-existing fissures under uniaxial compression," *Canadian Geotechnical Journal*, vol. 55, pp. 1–45, 2018.
[20] M. Koohmishi, "Assessment of strength of individual ballast aggregate by conducting point load test and establishment of classification method," *International Journal of Rock Mechanics and Mining Sciences*, vol. 141, 2021.
[21] H. Haeri, A. Hedayat, V. Sarfarazi, and A. Hedayat, "A review paper about experimental investigations on failure behaviour of non-persistent joint," *Geomechanics and Engineering*, vol. 13, no. 4, pp. 535–570, 2017.
[22] H. Haeri, "Experimental crack analyses of concrete-like CSCBD specimens using a higher order DDM," *Computers and Concrete*, vol. 16, no. 6, pp. 881–896, 2015.
[23] V. Sarfarazi, H. Haeri, A. B. Shemirani, and Z. Zhu, "Shear behavior of non-persistent joint under high normal load," *Strength of Materials*, vol. 49, no. 2, pp. 320–334, 2017.
[24] H. Haeri and V. Sarfarazi, "The deformable multilaminate for predicting the Elasto-Plastic behavior of rocks," *Computers and Concrete*, vol. 18, no. 2, pp. 201–214, 2016.
[25] A. Kumar, "The effect of stress rate and temperature on the strength of basalt and granite," *Geophysics*, 1968.
[26] F. R. Bunshah, *Techniques of Metals Research*, Interscience Publishers, Geneva, Switzerland, 1968.
[27] Z. Zhou, X. Cai, X. Li, W. Cao, and X. Du, "Dynamic response and energy evolution of sandstone under coupled static-dynamic compression: insights from experimental study into deep rock engineering applications," *Rock Mechanics and Rock Engineering*, vol. 53, no. 3, pp. 1305–1331, 2020.
[28] X. Cai, C. Cheng, Y. Zhao, Z. Zhou, and S. Wang, "The role of water content in rate dependence of tensile strength of a fine-grained sandstone," *Archives of Civil and Mechanical Engineering*, vol. 22, no. 1, pp. 1–16, 2022.
[29] W. Janach, "The role of bulking in brittle failure of rocks under rapid compression," *International Journal of Rock Mechanics and Mining Sciences & Geomechanics Abstracts*, vol. 13, no. 6, pp. 177–186, 1976.
[30] S. J. Green and R. D. Perkin, "Uniaxial compression tests at varying strain rates on three geologic materials," *Basic and Applied Rock Mechanics*, vol. 3, pp. 35–52, 1970.
[31] D. E. Logan and J. Handin, "Triaxial compression tests at intermediate strain rates," in *Dynamic Rock Mechanics*, G. B. Clark, Ed., pp. 167–194, Port city press, Baltimore, MA, USA, 1970.
[32] H. Kolsky, "An investigation of the mechanical properties of materials at very high rates of loading," *Proceedings of the Physical Society Section B*, vol. 62, no. 11, pp. 676–700, 1949.
[33] X. B. Li, T. S. Lok, and J. Zhao, "Dynamic characteristics of granite subjected to intermediate loading rate," *Rock Mechanics and Rock Engineering*, vol. 38, no. 1, pp. 21–39, 2005.
[34] R. J. Christensen, S. R Swanson, W. S. Brown, S. R. Swanson, and W. S. Brown, "Split-Hopkinson-bar tests on rock under confining pressure," *Experimental Mechanics*, vol. 12, no. 11, pp. 508–513, 1972.
[35] W. Goldsmith, J. L. Sackman, C. Ewerts, J. L. Sackman, and C. Ewerts, "Static and dynamic fracture strength of Barre granite," *International Journal of Rock Mechanics and Mining Sciences & Geomechanics Abstracts*, vol. 13, no. 11, pp. 303–309, 1976.
[36] W. A. Olsson, "The compressive strength of tuff as a function of strain rate from 10−6 to 103/sec," *International Journal of Rock Mechanics and Mining Sciences & Geomechanics Abstracts*, vol. 28, no. 1, pp. 115–118, 1991.
[37] W. S. Chang, "Impact of solid missiles on concrete barriers," *Journal of the Structural Division*, vol. 108, 1981.
[38] A. Haldar and H. A. Hamieh, "Local effect of solid missiles on concrete structures," *Journal of Structural Engineering*, vol. 110, no. 5, pp. 948–960, 1984.
[39] J. N. Goodier, *On The Mechanics Of Indentation And Cratering In Solid Targets Of Strain-Hardening Metal By Impact Of Hard And Soft Spheres*, Stanford Research Institute, Menlo Park, CA, USA, 1964.
[40] M. J. Forrestal, B. S. Altman, J. D. Cargile, and S. J. Hanchak, "An empirical equation for penetration depth of ogive-nose projectiles into concrete targets," *International Journal of Impact Engineering*, vol. 15, no. 4, pp. 395–405, 1994.
[41] M. J. Forrestal, D. J. Frew, S. J. Hanchak, and N. S. Brar, "Penetration of grout and concrete targets with ogive-nose steel projectiles," *International Journal of Impact Engineering*, vol. 18, no. 5, pp. 465–476, 1996.
[42] A. J. Piekutowski, M. J. Forrestal, K. L. Poormon, and T. L. Warren, "Penetration of 6061-T6511 aluminum targets by ogive-nose steel projectiles with striking velocities between 0.5 and 3.0 km/s," *International Journal of Impact Engineering*, 1999.